Journal of Fundamental and Applied Sciences

Research Article

ISSN 1112-9867

Available online at http://www.jfas.info

SYNTHESIS AND CHARACTERIZATION OF PEROVSKITE OXIDES $LaFe_{1-X}Cu_XO_3$ ($0 \leq X \leq 0.4$) OBTAINED BY SOL-GEL METHOD

A. Benaicha*, M. Omari

Laboratory of Molecular Chemistry and Environment, University of Biskra, BP 145, 07000 Biskra, Algeria

Received: 14 March 2017 / Accepted: 31 December 2017 / Published online: 01 January 2018

ABSTRACT

$LaFe_{1-x}Cu_xO_3$ (where *x* ranged from 0 to 0.4) powders are successfully synthesized by the sol-gel method employing metal nitrate salts as cations precursors and methanol as solvent. Thermogravimetric and differential thermal analysis (TGA/DTA) results exhibit that decomposition of the precursor to the oxide completed at about 750°C. XRD patterns exhibit that the materials belong to a cubic system. All samples show two IR active vibrational modes, one at 560 cm^{-1} assigned to Fe-O stretching vibration and another one at 1385 cm^{-1} assigned to the stretching of metal carbonates. SEM images of the samples show that the particle size is from 63 to 158 nm and the specific surface areas are relatively low. The electrochemical measurements exhibit that the catalytic activity is influenced by copper doping. The highest electrode performance is achieved with the oxide $LaFe_{0.7}Cu_{0.3}O_3$.

Keywords: perovskite oxide, sol-gel, thermogravimetric analysis, powder diffraction, electrochemical properties.

Author Correspondence, e-mail: koaicha@gmail.com

doi: http://dx.doi.org/10.4314/jfas.v10i1.9

1. INTRODUCTION

Many fields of modern chemical industry are based on the mixed metal oxides [1] including perovskite-type oxides (PTOs) [2] because of their high stability, excellent oxidation activity, their low price [3].They have various applications [4-7] thanks to their catalytic, optical,

magnetic, electronic and ferroelectric properties [8]. Perovskite-type oxides (PTOs) have the general formula ABO_3 [2] where A can be an alkali, alkaline earth, or lanthanide metal, B may be a 3d-transition metal [9]. The metal ions at A and/or B site can be partially substituted by other metal ions [10].

$LaFeO_3$ considered one of the important perovskite-type oxides (PTOs) [11] due to its various applications including environmental catalyst [12], fuel cells [13], chemical sensors [14], magnetic materials [15], and oxygen permeable membranes [6]. For the synthesizing of $LaFeO_3$, the literature mentions several synthesis methods, among those; solid-state oxide reaction method. It requires a high temperature, a long period, and unfortunately it produces uncontrolled particle size [11]. For better results, some alternative routes are proposed such as sol-gel method [9], sol-gel auto combustion [16], co-precipitation [17], microemulsion [18], hydrothermal method [19] and electrospinning method [12].

$LaFeO_3$ can be modified by the substitution of A and/or B sites which may affect strongly their physical properties. It was found that catalytic activities of $LaFe_{1-x}M_xO_3$ (M= Mn, Al, Co) complex oxides were much higher than that of $LaFeO_3$ sample because of the increase of the valence of B-site cations and lattice oxygen content [9]. In recent years, some studies of the system $LaFe_{1-x}Cu_xO_3$were conducted. First, Caronna et al. [20] have synthesized $LaFe_{1-x}Cu_xO_3$ oxides, where *x* ranged from 0 to 0.4 by citrate auto-combustion method and studied their structural characterization. They have obtained a solid solution in the composition range ($0 \leq x \leq 0.2$). Later, Prasad et al. [21] have prepared the orthorhombic $LaFe_{1-x}Cu_xO_3$ ($0 \leq x \leq 0.3$) perovskites by the sol-gel route and studied their dielectric and structural properties. Li et al. [22] have studied the effect of substitution of iron by copper ($0 \leq x \leq 0.3$) at $T \leq 500$ °C on the visible-light photocatalytic hydrogen evolution of $LaFeO_3$ oxide. The obtained XRD spectrum shows that there are two or three phases in all studied composition range. Recently, Parrino et al. [23] have prepared using the citrate autocombustion synthesis method, studied the photocatalytic activity in gas-solid regime beneath simulated solar light irradiation of Cu-doped $LaFeO_3$ in the composition range ($0 \leq x \leq 0.4$). They have concluded that the solubility limit is reached at $x = 0.2$

The purpose of our present work is to study the substitution effect of iron by copper on electrochemical, structural and morphological properties of $LaFe_{1-x}Cu_xO_3$ oxides ($0 \leq x \leq 0.4$) synthesized via sol-gel method.

2. EXPERIMENTAL

A series of the $LaFe_{1-x}Cu_xO_3$ perovskites (x=0-0.4) is synthesized using sol-gel method as reported earlier using starting materials $La(NO_3)_3.6H_2O$, $Fe(NO_3)_3.9H_2O$, $Cu(NO_3)_2.6H_2O$ and citric acid ($C_6H_8O_7.H_2O$). First, these starting materials are dissolved in methanol with the desired Fe/Cu ratio, the solution is slowly stirred, heated at 70 °C for about 2h up to the formation of a gel compound. Then, it is dried overnight at 100°C to obtain the dry precursors by evaporating the solvent. The precursors obtained have been ground into powders, then calcined with different calcination temperatures from 450°C to 850°C in air for 6h at heating rate of 5°C min^{-1}. Thermogravimetric (TG) and differential thermal analysis (DTA) have been carried out from room temperature to 1000°C in air at a heating rate of 10°C min^{-1} using a LINSEIS STA PT1600. The samples phase purity has been checked by recording X-ray data in the 2 theta range 10°-80° using a Brucker D8_Advance X-ray diffractometer. IR spectra are recorded by using FTIR_Shimadzu 8400S spectrometer. The BET surface areas of the powder calcined with different calcination temperatures have been realized by using Quantachrome Instruments (version.2.13). SEM photographs are taken in order to examine the particle morphology of the perovskite by using a QUANTA FEG 450 scanning electron microscope. The electrochemical experiments for O_2 evolution and methanol oxidation are performed by using a Volta Lab 40 potentiostat/galvanostat. The measurements have been carried out in a three-comportment cell. Potassium hydroxide electrolyte solution (1M) has been prepared by dissolving a required amount of KOH (Merck) in bidistilled water. The working electrodes ($1cm^2$) have been obtained by painting with an oxide suspension. The counter has been Hg/HgO/1M KOH. All potentials in the text have been referred to this reference electrode.

3. RESULTS AND DISCUSSIONS

3.1. TG/DTA analysis of the precursor

A typical TG/DTA curve of $LaFe_{0.8}Cu_{0.2}O_3$ precursor gel with heating rate of a 10°C min^{-1} from 25°C to 1000°C is shown in Fig.1 According to major changes observed on the TG graph, we can divide the decomposition process into three steps (25-250°C, 250-550°C, 550-820°C).

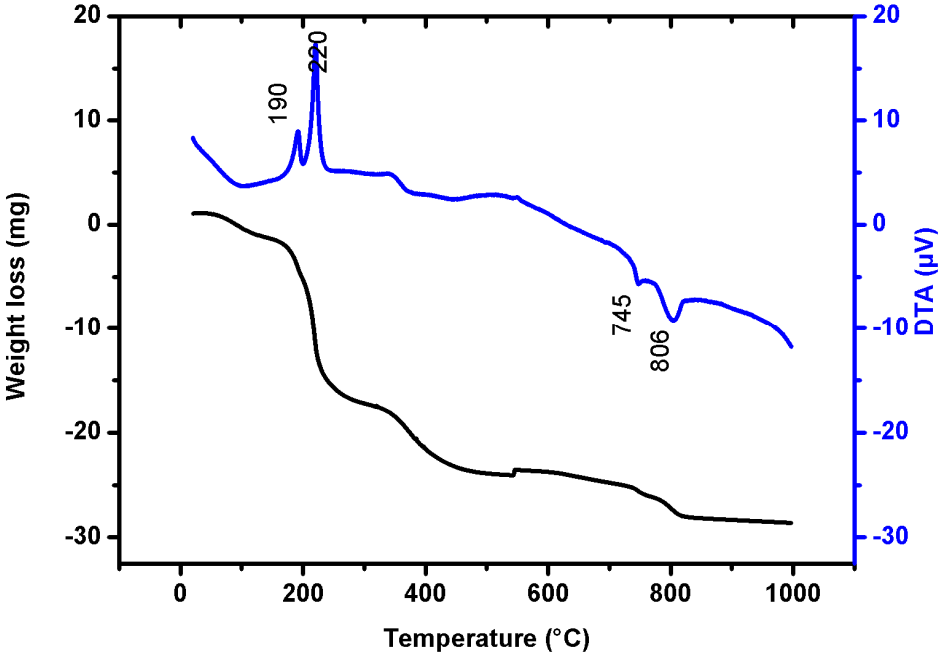

Fig.1. TG and DTA curves of $LaFe_{0.8}Cu_{0.2}O_3$ precursor heated in air at 10°C min^{-1}

The mass loss of $LaFe_{0.8}Cu_{0.2}O_3$ precursor gel powder corresponding to the first step until 250°C is associated with a water desorption and organic substances decomposition (methanol, citric acid), also reflected by two exothermic peaks at 190 and 220°C in DTA curve [24]. The second mass loss between 250-550°C associated to a broad and weak endothermic peak appearing in the same range of temperature in DTA curve, may be regarded as a result of the burning of the remaining organic materials accompanied by evolution of CO_2 and H_2O gases and the formation of a metal carbonate [25]. The mass loss in the third step between 720-820°C probably attributed to the formation of $LaFe_{0.8}Cu_{0.2}O_3$ oxide is associated with two exothermic peaks at 745°C and 806°C as seen in DTA curve [26], confirmed by XRD results discussed below.

3.2. IR analysis of the calcined samples

FT-IR analysis of the calcined samples is important both for the properties of the obtained materials and control the process of the reaction. Fig.2 shows the infrared spectra of $LaFe_{0.8}Cu_{0.2}O_3$ sample heated at different temperatures from 450 to 850 °C. The spectra of the sample $LaFe_{0.8}Cu_{0.2}O_3$ are similar. The strong absorption band observed at 560 cm^{-1} is attributed to Fe-O stretching vibration [27], which confirms the formation of the perovskite. The absorption band at 1385 cm^{-1} owing to the splitting of v_3 asymmetric stretching of metal carbonates [1] is gradually decreasing with increasing temperature until it disappeared in the sample heated at 850°C.For the sample heated at 450 °C, a broad absorption band is observed

at about 3405 cm^{-1} which is assigned to O-H stretching [28], whereas the band at 560 cm^{-1}has weakly appeared, which indicates a partial formation of the oxide at this temperature.

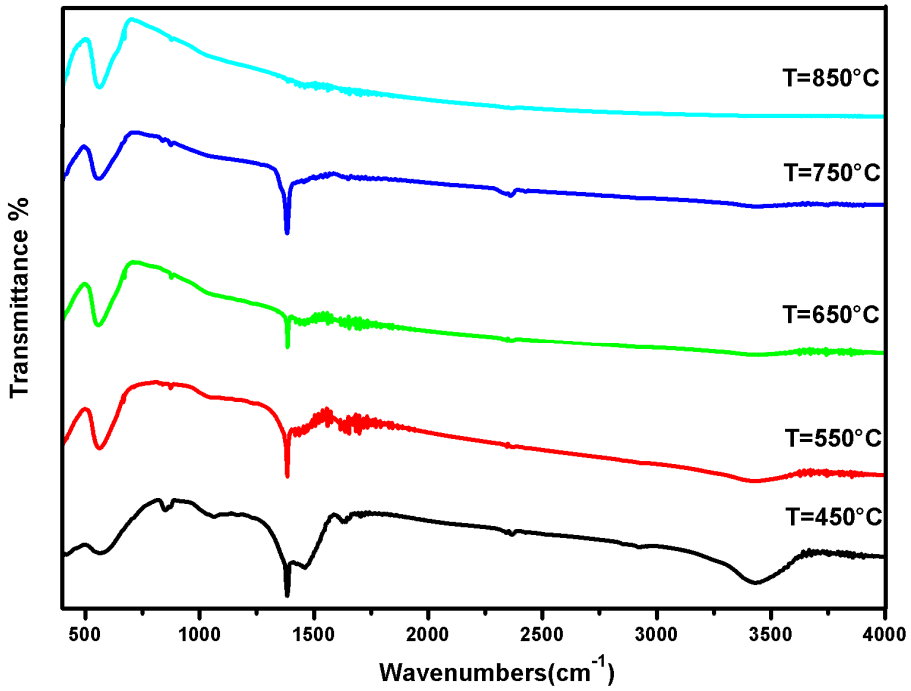

Fig.2. Infrared spectra of $LaFe_{0.8}Cu_{0.2}O_3$ powder sample calcined at different temperatures

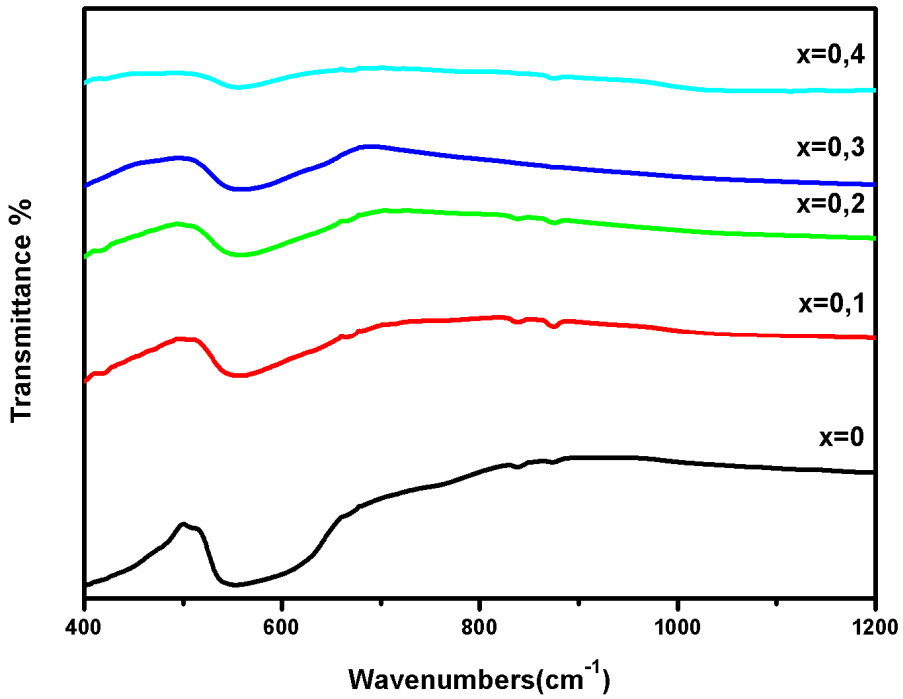

Fig.3. Infrared spectra of the $LaFe_{1-x}Cu_xO_3$ perovskites ($0 \leq x \leq 0.4$) samples calcined at different calcination temperatures

The infrared spectra of $LaFe_{1-x}Cu_xO_3$ ($0 \leq x \leq 0.4$) samples heated at 750-850 °C Fig.3. In each case, the band of Fe-O stretching vibration at 560 cm^{-1} is observed which confirms clearly the formation of the perovskite structure.

3.3. XRD analysis

Fig.4 shows the XRD patterns of the calcined powders $LaFe_{1-x}Cu_xO_3$ ($0 \leq x \leq 0.4$) obtained by sol-gel route after 6h of calcination at 750-850 °C. The results reveal that all $LaFe_{1-x}Cu_xO_3$ samples have a perovskite-type structure with no detectable secondary phase; therefore, all the main diffraction peaks could be indexed in the cubic system (JCPDS card 75-0541). These results indicate also that the structure of the perovskite is well maintained after substitution of iron by copper and the solubility limit is reached at x=0.4.

Fig.5 shows the XRD patterns of $LaFe_{0.8}Cu_{0.2}O_3$ powders calcined at different calcination temperatures (450-850 °C) for 6h. An amorphous system is obtained for the sample heated at 450 °C. The XRD patterns of the $LaFe_{0.8}Cu_{0.2}O_3$powders heated at 550 and 650°C reveal that the presence of three crystalline phases. A cubic phase (JCPDS card 75-0541) with poor crystallinity, La_2O_3 (JCPDS card 074-1144) and Fe_3O_4 (JCPDS card 075-0449) phases. Peak diffractions of the last two phases decreased at 650°C, disappeared completely in the XRD patterns at 750 and 850°C and only a single cubic phase (JCPDS card 75-0541) remains present with good crystallinity.

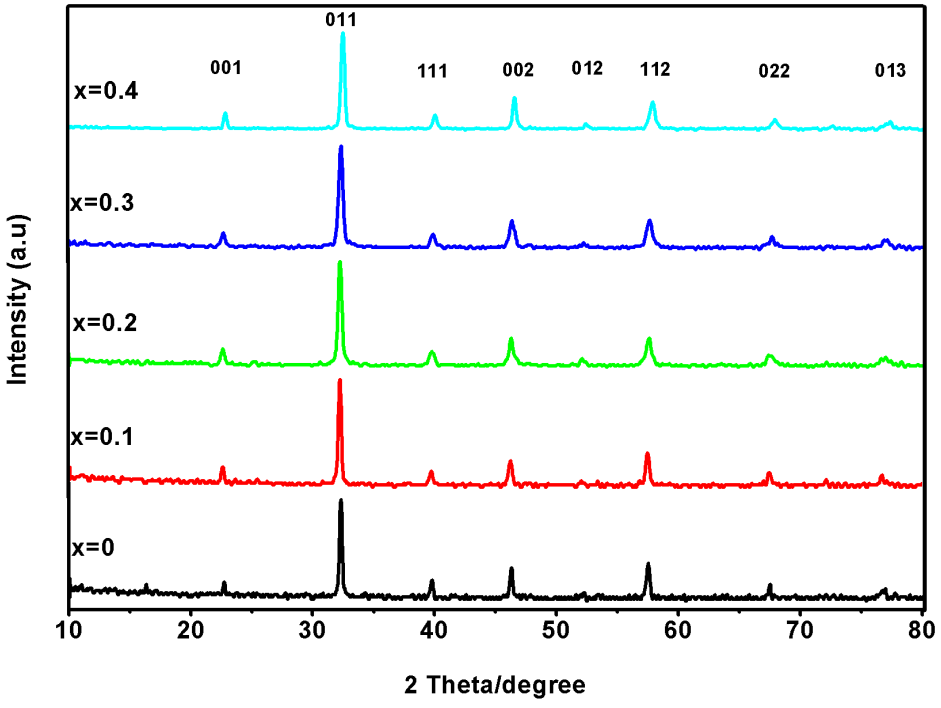

Fig.4. X-ray diffraction patterns of perovskite samples $LaFe_{1-x}Cu_xO_3$ ($0 \leq x \leq 0.4$)

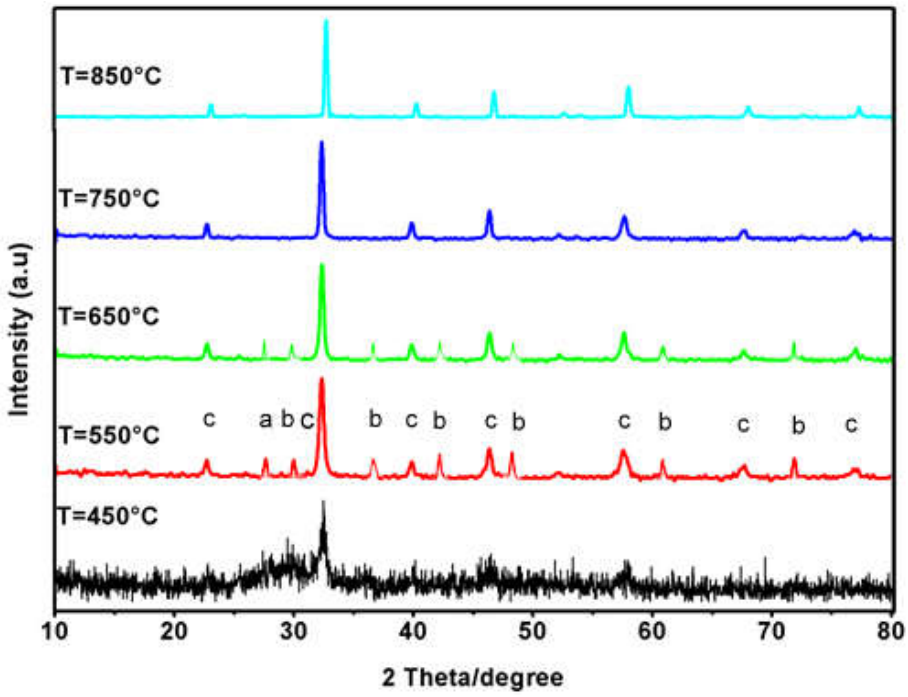

Fig.5. X-ray diffraction patterns of the $LaFe_{0.8}Cu_{0.2}O_3$ powder calcined with different temperatures**:** (a) La_2O_3; (b) Fe_3O_4; (c) cubic phase

The lattice parameters of the perovskites $LaFe_{1-x}Cu_xO_3$ have been calculated for each *x* value from the XRD patterns using Celref programme Fig.6. We can observe that the volume decreases when Cu content increases in the sample (due to the substitution of the larger Fe ions by the smaller Cu ions). The straight line means that a solid solution was formed in the composition range ($0 \leq x \leq 0.4$).

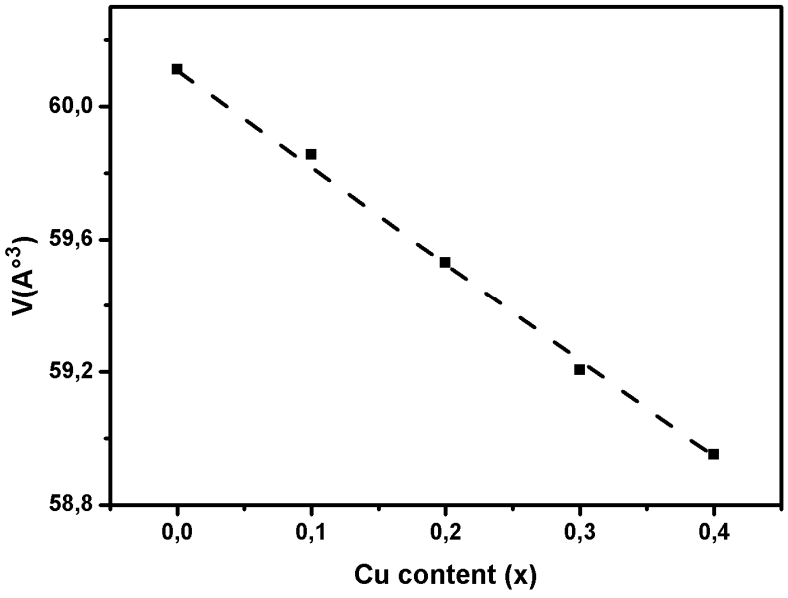

Fig.6. Lattice volume dependence on copper content (x) for $LaFe_{1-x}Cu_xO_3$

3.4. Specific surface area analysis (BET)

Table.1 represents the BET-surface area, pore diameter, and particle size results of the calcined powders $LaFe_{1-x}Cu_xO_3$ ($0 \leq x \leq 0.4$). The smallest particle size (63.4 nm) gives the best specific surface area (6.7 m^2 g^{-1}) and the bigger gives the lower specific surface areas. It is known that the particle size and surface area are related to each other inversely [29] and our results are in agreement with this concept. In general, our results show that the specific surface areas of the prepared powders were low and that is may be because of the high calcination temperature (from 750°C to 850°C). It is very well known that the specific surface area of perovskite is affected by the calcination temperature [2].

Table 1. BET surface area, average pore diameter and average particle size of $LaFe_{1-x}Cu_xO_3$

The samples	BET-surface area (m^2 g^{-1})	Average Pore diameter (Å)	Average Particle size (nm)
X=0	2.9	87.8	97.0
X=0.1	4.6	96.2	78.5
X=0.2	6.7	156.4	63.4
X=0.3	1.7	59.1	126.9
X=0.4	0.5	113	158

3.5. SEM analysis

The SEM micrographs of the calcined powders $LaFe_{1-x}Cu_xO_3$ ($0 \leq x \leq 0.4$) are presented in Fig.7. The powders are observed to be compact and few volatile grains which leave pores in material due to escaping gases from the decomposition of organic compounds and the strong redox reaction during the formation of perovskites [16]. pores are seen clearly in SEM images of the powders (x=0, 0.1, and 0.2) with decreasing of particle size (from 97 to 63 nm) respectively, which explain the high specific surface areas for these compositions. By seeing SEM micrographs of the samples (x=0.3, and x=0.4) where the formation of the big grains with decreasing of pores, we can understand why they give low specific surface areas.

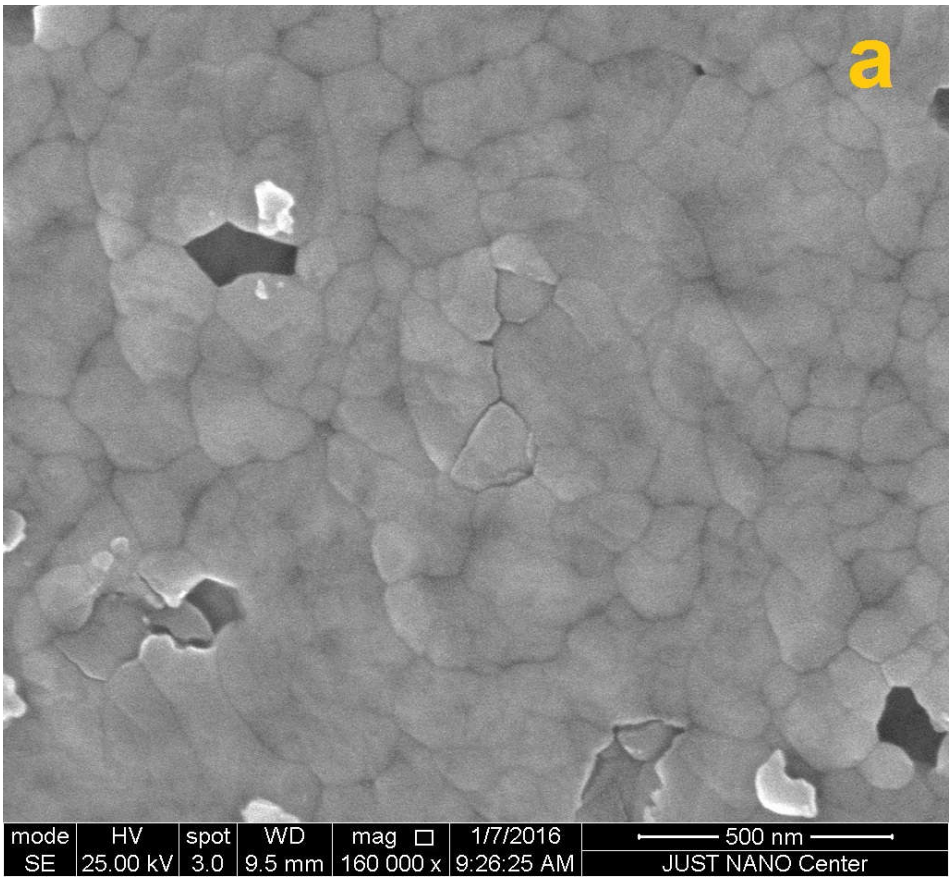
a
mode HV spot WD mag 1/7/2016 500 nm
SE 25.00 kV 3.0 9.5 mm 160 000 x 9:26:25 AM JUST NANO Center

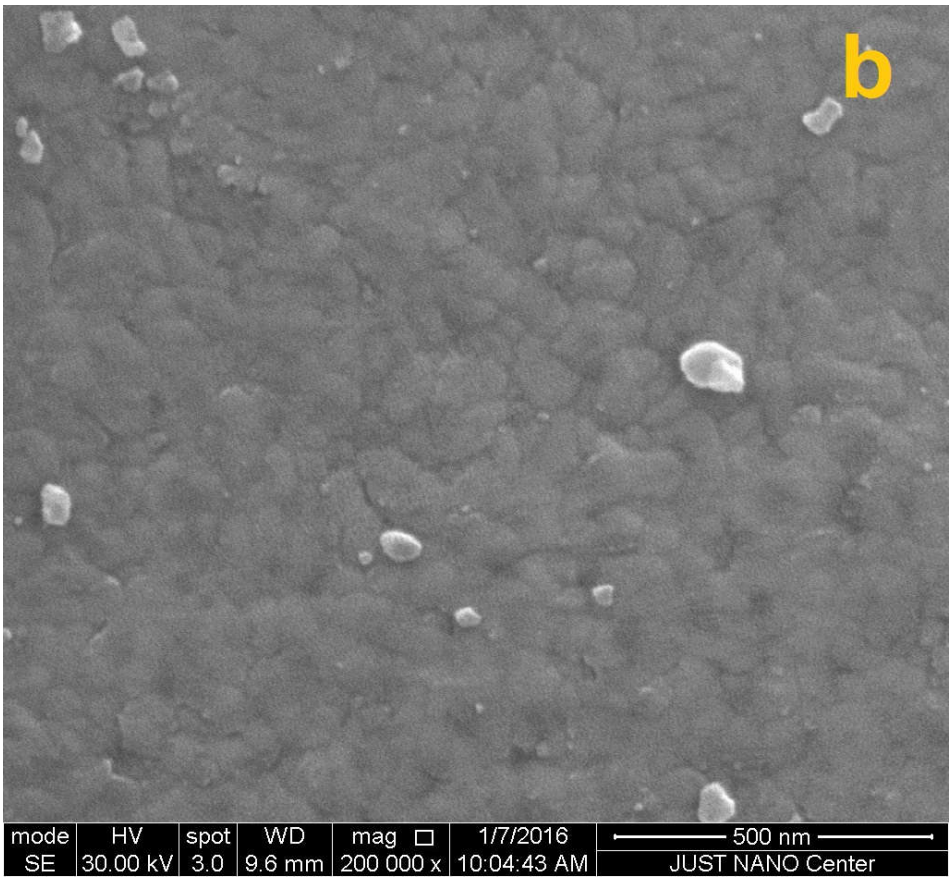
b
mode HV spot WD mag 1/7/2016 500 nm
SE 30.00 kV 3.0 9.6 mm 200 000 x 10:04:43 AM JUST NANO Center

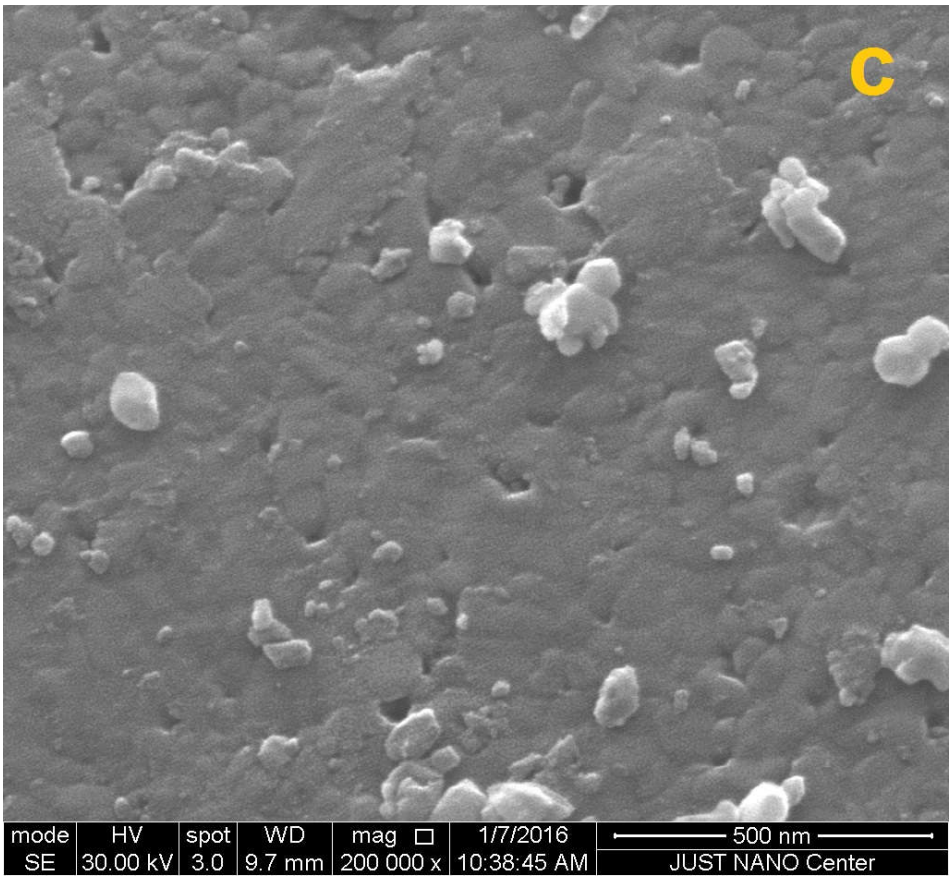
c
mode HV spot WD mag 1/7/2016 500 nm
SE 30.00 kV 3.0 9.7 mm 200 000 x 10:38:45 AM JUST NANO Center

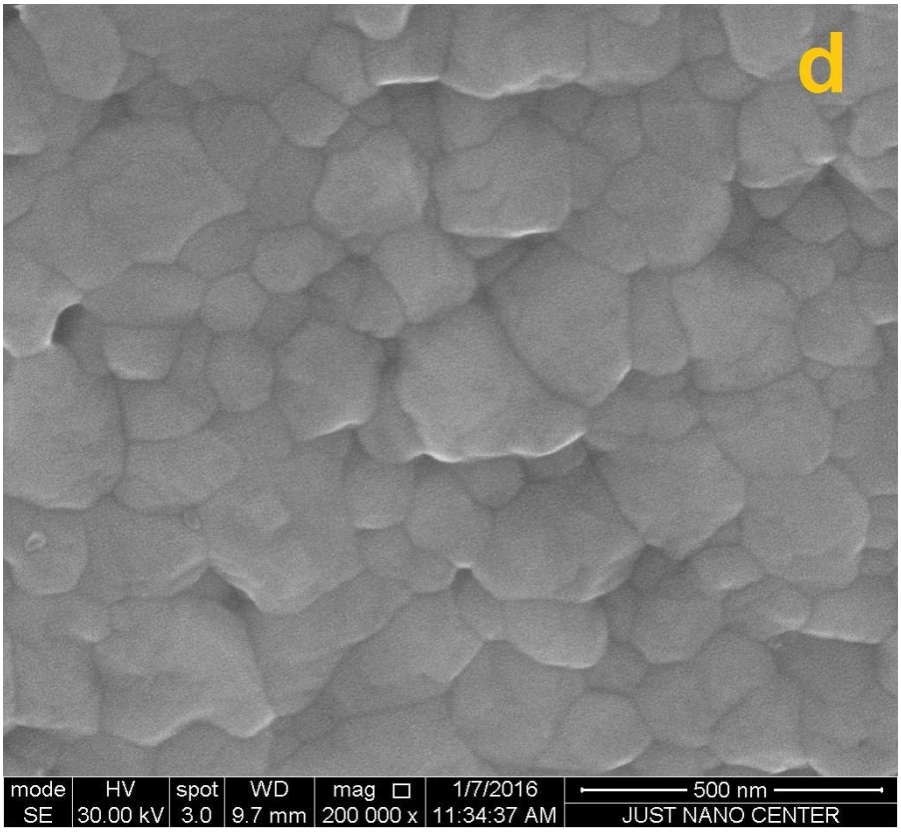
d
mode HV spot WD mag 1/7/2016 500 nm
SE 30.00 kV 3.0 9.7 mm 200 000 x 11:34:37 AM JUST NANO CENTER

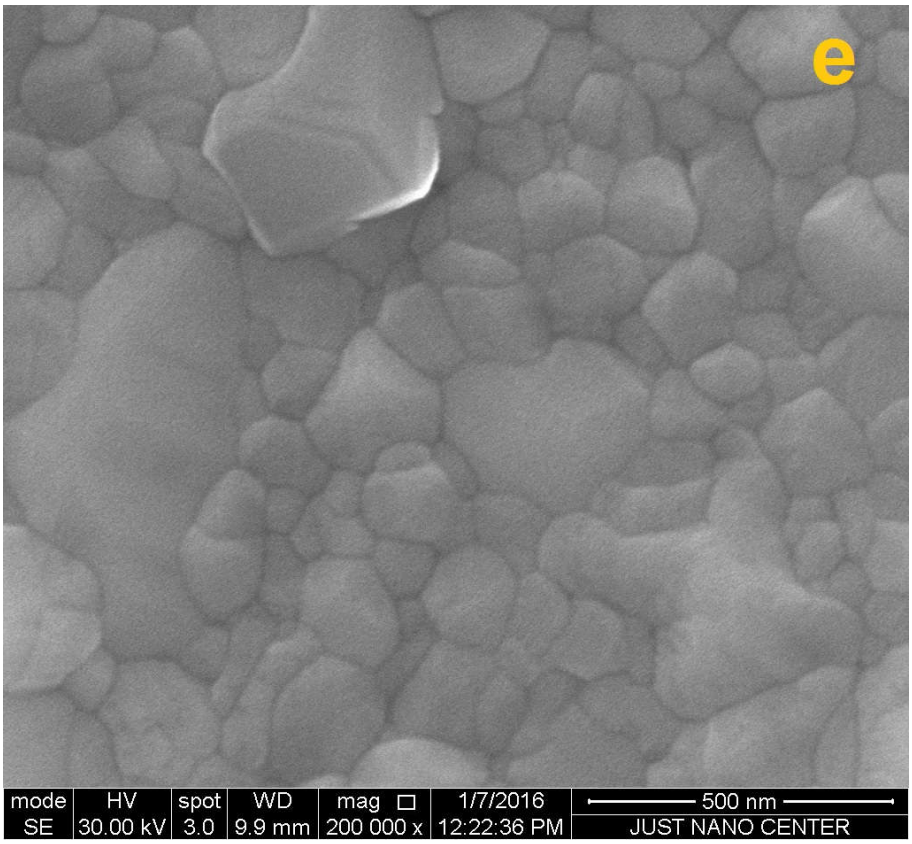

Fig.7. SEM micrographs of $LaFe_{1-x}Cu_xO_3$**: a** x=0, **b** x=0.1, **c** x=0.2, **d** x=0.3 and **e** x=0.4

3.6 Electrochemical Properties

The electrochemical activity for oxygen evolution reaction was investigated on $LaFe_{1-x}Cu_xO_3$ coated nickel substrate according to:

$$O_2 + 2H_2O + 4e^- \leftrightarrow 4OH^-$$

Polarization studies under potentiostatic conditions were carried out. Fig.8 shows the cathodic and anodic current–potential curves of air electrode with different substitutions of copper in KOH(1M). The voltammograms exhibit two redox peaks, an anodic (Epa =544 mV) and a corresponding cathodic (Epc =402 mV) peak, prior to the onset of the O_2 evolution reaction, revealing a pseudocapacitance because of the Ni(III)/Ni(II) surface redox couple [30, 31].

Compounds with large copper content show higher anodic currents than those with smaller x. Compared to all compositions, the $LaFe_{0.7}Cu_{0.3}O_3$ one seems to be the most active. Copper, a divalent cation increases the catalytic activity and provides a catalyst with high structural stability due to the essential role of the transition metal ion in developing highly active catalysts. At the same voltage, the highest electrode performance is achieved for oxygen evolution with x=0.3, (i_a=14.3 µA.cm^{-2} at Epa =544 mV).

Fig.9 shows the anodic current–potential curves of air electrode with different substitutions of copper in KOH(1M)+CH_3OH(1M). The voltammograms exhibit an anodic peak (Epa =876 mV), but no cathodic peak in this medium. The voltammetric profile is rather featureless, showing a wide plateau region. It is clear that the coated perovskite electrodes present a wide range of electrochemical stability and a composition dependency of the current intensity Compounds with large copper content show higher anodic currents than those with smaller x. Compared to all compositions, the $LaFe_{0.7}Cu_{0.3}O_3$ one seems to be the most active, (i_a=32.6 µA.cm^{-2} at Epa =876 mV).

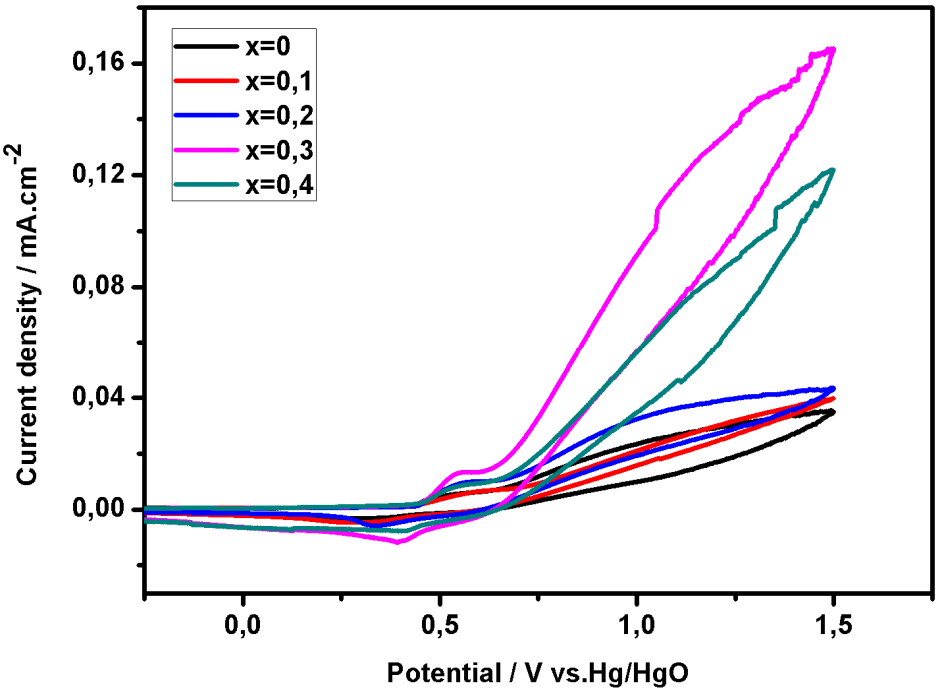

Fig.8. Cathodic and anodic polarization curves for $LaFe_{1-x}Cu_xO_3$ electrodes in 1 M KOH

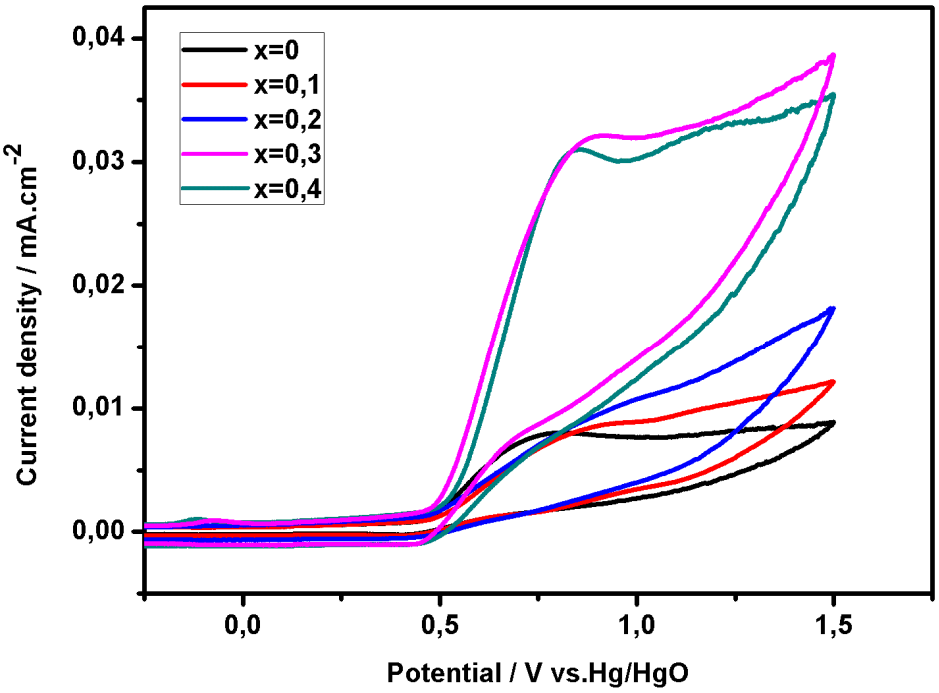

Fig.9. Cathodic and anodic polarization curves for $LaFe_{1-x}Cu_xO_3$ electrodes in KOH(1M)+CH_3OH(1M)

4. CONCLUSIONS

Perovskite-type $LaFe_{1-x}Cu_xO_3$ ($0 \leq x \leq 0.4$) oxides are successfully synthesized by sol-gel route employing metal nitrate salts as cations precursors. Structural characterization showed that the structure had a single phase of cubic perovskite, formed in a heating at about 750°C in air for 6h. The microstructure and morphology of the compounds exhibited that the copper content affects the surface area that leads the material compact with decreasing of pores. Compared to all studied compositions, $LaFe_{0.7}Cu_{0.3}O_3$ electrode exhibits significantly greater electroactivity, indicating that this material is among the analyzed series the best electrocatalyst for oxygen evolution.

5. REFERENCES

[1] Abazari R and Sanati S 2013 Superlattices and Microstructures **64** 148-157.

[2] Fang Y Z, Liu Y and Zhang L H 2011 Applied Catalysis A: General **397** 183-191.

[3] Labhasetwar N, Saravanan G, Megarajan S K, Manwar N, Khobragade R, Doggali P and Grasset F 2015 Sci. Technol. Adv. Mater. **16** 036002

[4] Kaiwen Z, Xuehang W, Wenwei W, Jun X, Siqi T and Sen L 2013 Advanced Powder Technology **24** 359.

[5] Nie Y, Zhang L, Li Y Y, Hu C 2015 Journal of Hazardous Materials **294** 195–200.

[6] Pushpa R, Daniel D and Butt D P 2013 Solid State Ionics **249–250** 184–190.

[7] Khetre S M, Chopade A U, Khilare C J and Bamane S R 2011 International Journal of Porous Materials **1(1)** 1-5.

[8] Shikha P, Kang T S and Randhawa B S 2015 Journal of Alloys and Compounds **625** 336–345.

[9] Orge C A, Órfão J J M, Pereira M F R, Barbero B P and Cadús L E 2013 Applied Catalysis B: Environmental **140– 141** 426– 432.

[10] Lafuerza S, Subias G, Garcia J, Matteo S D, Blasco J, Cuartero V and Natoli C R 2011 J. Phys. Condens. Matter. **23** 325601.

[11] Gosavi P V and Biniwale R B 2010 Materials Chemistry and Physics **119** 324–329.

[12] Leng J, Li S, Wang Z, Xue Y and Xu D 2010 Materials Letters **64** 1912–1914.

[13] Coffey G, Hardy J, Marina O, Pederson L, Rieke P and Thomsen E 2004 Solid State Ionics **175** 73–78.

[14] Phokha S, Pinitsoontorn S, Rujirawat S and Maensiri S 2015 Physica B: Condensed Matter. **476** 55–60.

[15] Lee W Y, Yun H J and Yoon J W 2014 Journal of Alloys and Compounds **583** 320–324.

[16] Parida K, Reddy K, Martha S, Das D and Biswal N 2010 International Journal of Hydrogen Energy **35** 12161-12168.

[17] Djoudi L and Omari M 2015 J. Inorg. Organomet. Polym. **25**, 796.

[18] Li F, Liu Y, Liu R, Sun Z, Zhao D and Kou C 2010 Materials Letters **64** 223-225.

[19] Nikam S K and Athawale A A 2015 Materials Chemistry and Physics **155** 104-112.

[20] Caronna T, Fontana F, Natali Sora I and Pelosato R 2009 Mater. Chem. Phys. **116** 645–648.

[21] Prasad B V, Rao B V, Narsaiah K, Narsinga R G, Chen J W and Babu D S 2015 Materials Science and Engineering **73** 012129.

[22] Li J, Pan X, Xu Y, Jia L, Yi X and Fang W 2015 International Journal of Hydrogen Energy **40** 13918-13925.

[23] Parrino F, García-López E, Marcì G, Palmisano L, Felice V, Natali Sora I and Armelao L 2016 Journal of Alloys and Compounds **682** 686-694.

[24] Shabbir G, Qureshi A H and Saeed K 2006 Materials Letters **60** 3706–3709.

[25] Banerjee K, Mukhopadhyay J, Barman M and Basu R N 2015 Materials Research Bulletin **72** 306–315.

[26] Brunckova H, Medvecky L, Briancin J, Durisin J, Mudra E, Sebek M, Kovalcikova A and Sopcak T 2016 Materials Letters **165** 239–242.

[27] Kumar M, Srikanth S, Ravikumar B, Alex T C and Das S K 2009 Materials Chemistry and Physics **113(2)** 803-815.

[28] Hou L, Sun G, Liu K, Li Y and Gao F 2006 J. Sol–Gel Sci. Technol. **40** 9-14.

[29] Li Z, Chen G, Tian X and Li Y 2008 Mater. Res. Bull. **43** 1781-1788.

[30] Singh R N, Koenig J F, Poillerat G and Chartier P 1990 J. Electrochem. Soc. **137** 1408-1413.

[31] AbdelRahim M A, AbdelHameed R M and Khalil M W 2004 J. Power Sources **134** 160-169.

How to cite this article:
Benaicha A, Omari M. Synthesis and characterization of perovskite oxides $lafe_{1-x}cu_xo_3$ ($0 \leq x \leq 0.4$) obtained by sol-gel method. J. Fundam. Appl. Sci., 2018, *10(1), 132-146.*